

*115-124*

## Theoretical and Experimental Investigation of the Channeling Effect in Fluid Flow through Porous Media

M. R. Shahnazari\* and M. Zia Bashar Hagh

Mechanical Engineering Department,  
K. N. Toosi University of Technology, Tehran, Iran  
E-mail: mshahnazari@nri.ac.ir

### ABSTRACT

*During fluid flow through a channel filled with porous fiber, due to the gap between the walls and the edge of fiber or the variation of porosity, permeability will become a variable. In this paper, an exponential model is assumed for porosity and permeability. Also, the two-dimensional momentum equation is solved by the finite difference method, using a marker and cell (MAC) scheme and variable grid size mesh. Also, in order to verify the theoretical results, an experimental apparatus is designed and constructed. The experimental results were used to determine the model parameters. The results showed good validity of the assumed exponential model for prediction of preformed fiber permeability with air gap, as a function of distance from the walls.*

## NOMENCLATURE

$B$	gap width between wall and edge of fiber, m
$H$	half-height of channel, m
$K$	permeability, $m^2$
$P$	pressure, Pa
$t$	time, sec
$u$	in-plane velocity, m/sec
$U$	velocity vector
$v$	normal velocity, m/sec
$x$	in-plane direction
$y$	normal direction

### Greek symbols

$\alpha$	parameter in variable permeability equation
$\beta$	parameter in variable permeability equation
$\rho$	density, $kg/m^3$
$\epsilon$	porosity

### Subscripts

$f$	fluid
$o$	outlet
$\infty$	bulk properties

## 1. INTRODUCTION

Investigation of transport phenomena in porous media is important due to variety of different industrial applications. In some applications, such as fixed-bed catalytic reactors, packed-bed heat exchangers, drying, and resin injection molding, the constant-porosity assumption does not hold, because of the influence of an impermeable boundary.

The variable porosity close to an impermeable boundary leads to a number of important effects such as flow maldistribution and channeling. Channeling, which refers to the occurrence of maximum velocity in a region close to an external boundary, has been reported by many investigators, namely, Schwartz and Smith (1953) and Schertz and Bischoff (1969). Their velocity measurements in packed beds show a maximum value at regions close to the boundary. Furthermore, the measurements of Roblee et al. (1958) and Benenati and Brosilow (1962) show a distinct porosity variation in a packed bed. Their results show a high-porosity region close to the external boundary. The porosity, as a function of the distance from the boundary, can be obtained from these measurements. Vafai (1986) analyzed the effects of variable porosity on convective flow in porous media. The qualitative effects of controlling parameters on flow in variable-porosity media are discussed in his work. The high porosity near the edges has also been investigated by Bickerton and Advani (1995). They used a one-dimensional mold for systematic experimental study of the role of air in mold filling time.

In order to describe the channeling effect, the flow front position should be investigated. The surface enhancement in a fluid porous media has been investigated by Srinivasan and Vafai (1994). They presented an analytical solution for this problem.

Also, Chen and Vafai (1996) have studied two-dimensional flow of a porous medium with constant porosity in a duct, using the marker and cell (MAC) method. Shahnazari and Abbassi (2004) also used this method by inclusion of an irregular grid mesh and a trial-and-error scheme to predict the free surface position in a porous medium with variable porosity.

In this paper, a numerical and experimental investigation of the channeling effect on fluid flow through a porous media is presented. The experimental results have been compared with numerical model results to determine the permeability's exponential function coefficients.

## 2. EXPERIMENTAL APPARATUS

The experimental system was constructed to inject resin at a constant pressure (Fig. 1). A mold cavity with dimensions of  $25 \times 42 \times 1$  cm was designed in order to saturate the porous medium. Figure 2 shows the entry region before the fluid comes into contact with the porous media, which is 2 cm long.

Experiments were performed using a mixture of 67% glycerin and 33% ethylene glycol. This combination provides a viscosity around 200–220 cP at room temperature.

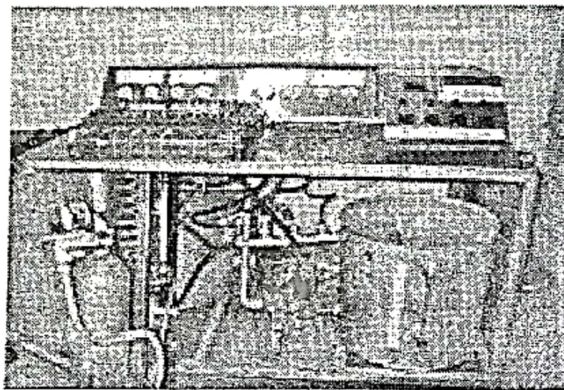
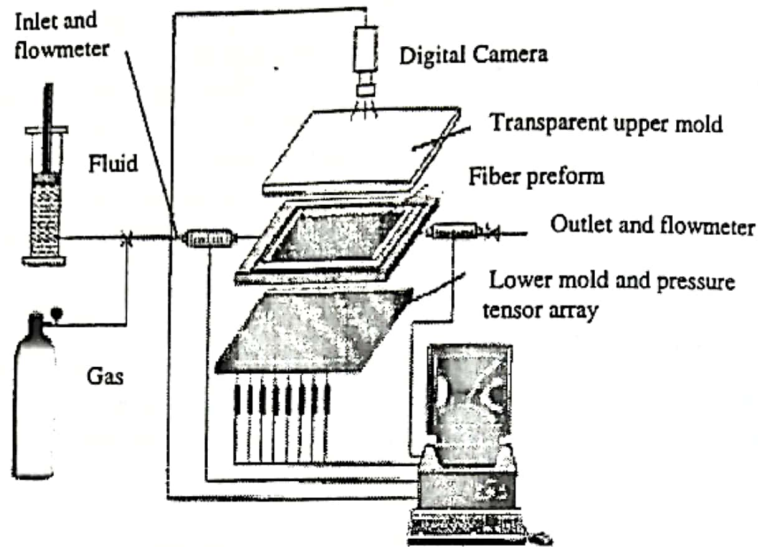


Figure 1. The experimental apparatus.

The portable ultrasonic flow meter (Fluxus ADM 6225) was used to measure the mass flow rate. The accuracy of this flow meter is  $\pm 0.5\%$  of the reading and its resolution is 0.025 cm/s. Tests were conducted in a mold with a Plexiglas top plate in order to observe the flow during the injection process.

Flow pressure during the injection was measured by pressure gauges. Two types of preformed fibers were used as porous media (Fig. 3). The fibers' porosity and permeability were evaluated by direct and adaptive experimental method by Yoon et al. (1998). In order to investigate the channeling effect, at each inlet pressure, the tests were conducted for a different gap width between the preformed edge and mold wall, which is shown in Fig. 4.

### 3. GOVERNING EQUATIONS

As mentioned earlier, the system comprises a horizontal channel, which is filled with porous material. It was assumed that the variation of porosity in the  $y$  direction changes exponentially.

The governing equations are as follows (Shahnazari and Abbassi, 2004):

$$\frac{\partial u}{\partial x} + \frac{\partial v}{\partial y} = 0 \tag{1}$$

$$\frac{-\epsilon}{\rho_f} \nabla p_f + \frac{\mu_f}{\rho_f} \nabla^2 U - \frac{\mu_f \epsilon U}{K \rho_f} = 0 \tag{2}$$



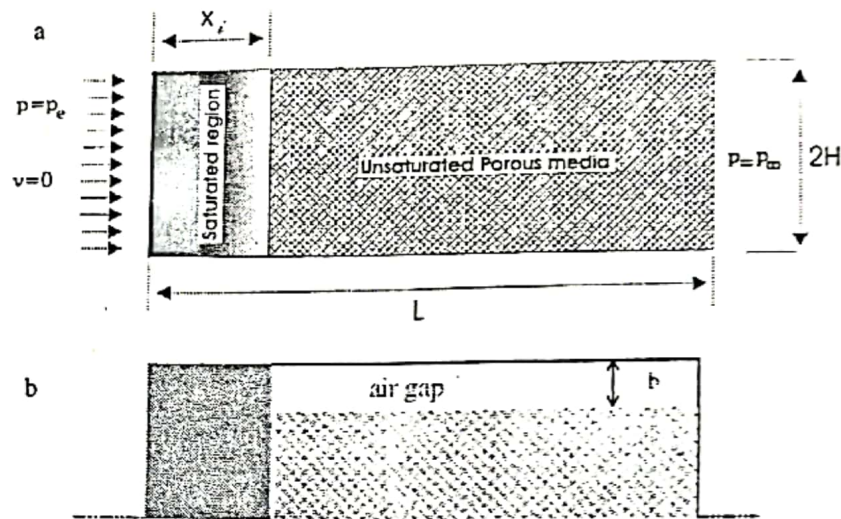
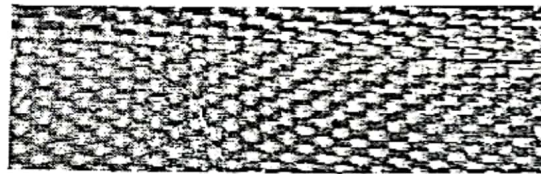
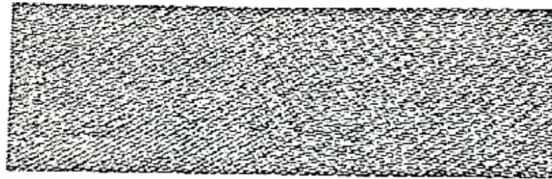


Figure 2. Entry region: a) mold geometry and b) air gap location.



(a)- E-glass uni. fiber I



(a)- E-glass uni. fiber II

Figure 3. Preformed fibers used in the tests.

Also, the boundary conditions at the entrance and the interface are as follows:

$$P = P_e, \quad v = 0 \quad \text{at} \quad x = 0 \quad (3)$$

$$P = P_0, \quad \frac{\partial u}{\partial X} = 0 \quad \text{at} \quad x = x_0 \quad (4)$$

$$u = v = 0 \quad \text{at} \quad y = 0, 2H \quad (5)$$

$$u = v \quad \text{at} \quad t = 0 \quad (6)$$

To model a nonhomogeneous porous media, an exponential function for porosity and permeability (Vafai,

1986), and the combination of these models was used. As a result, the permeability coefficients can be shown in terms of bulk permeability values as follows:

$$K = K_\infty(1 + \alpha \exp(-\beta y)) \quad (7)$$

where  $K_\infty$ ,  $\alpha$ ,  $\beta$  are experimental coefficients.

In the momentum equation, Eq. (2), the Brinkman-Forchheimer term has not been considered, due to the low Reynolds number of the fluid flow. The marker and cell (MAC) method with irregular mesh was applied to determine the surface enhancement of the fluid (Shahnazari and Abbassi, 2004). A nonuniform grid, together a with

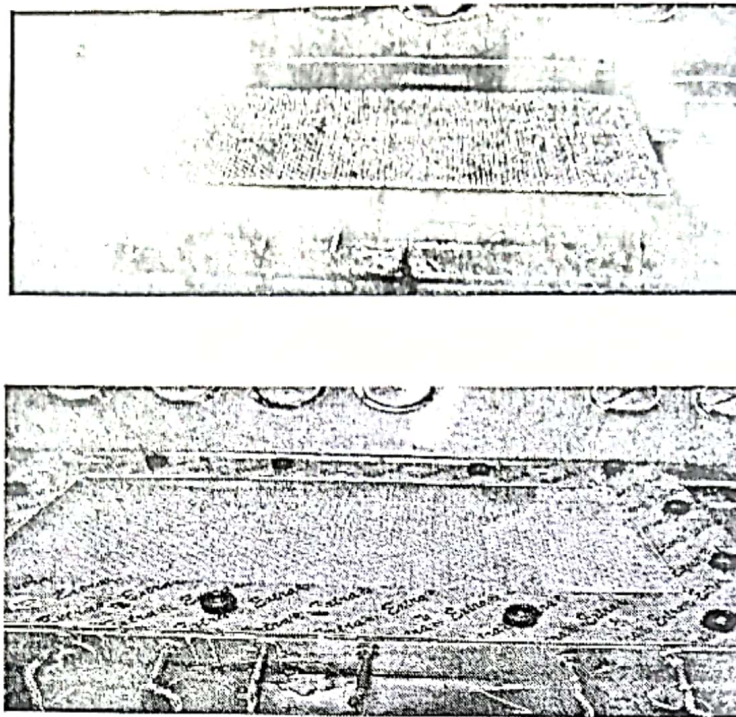


Figure 4. Experiments with air gap between the mold wall and the edge of the fiber.

higher-order finite difference approximation that uses the nearest and next-nearest neighbors, turned out to be very accurate.

#### 4. EXPERIMENTAL TESTS

##### 4.1. Bulk Permeability Prediction

In order to evaluate the preformed fiber's permeability, the mold fiber was filled by fluid flow at three constant-pressure gradient conditions. The average bulk permeability was calculated using direct and adaptive methods (see Appendix). Also, this calculation has been done at the saturation condition and advancing front flow.

The consistency between the simulation and experimental results depends on the measurement of the physical parameters such as viscosity, pressure, and permeability. Before starting the process, simulation parameters were measured accurately. Then, the model for constant permeability around the evaluated numerical results was solved. By comparing the experimental and numerical filling time, the average bulk permeability for each fiber was measured and are presented in Table 1.

Table 1  
Preformed fibers' permeability

Preformed fibers	Porosity (%)	Permeability (m <sup>2</sup> )
E-glass uni I	69	10 <sup>9</sup> × 1.7
E-glass uni II	51	10 <sup>-9</sup> × 0.8

##### 4.2. Variable Porosity Tests

Several experiments were conducted for each fiber with an air gap between the mold walls. Digital photos for each test were converted to metafiles and then the final results were converted into data files. Based on these data files for each point of mold height, the permeability values were calculated to evaluate the coefficients of Eq. (7).

#### 5. RESULTS AND DISCUSSIONS

Figure 5 shows the ratio of the permeability of a point with the maximum velocity (Kg) to the bulk permeability versus the nondimensional gap width. Based on the assumed



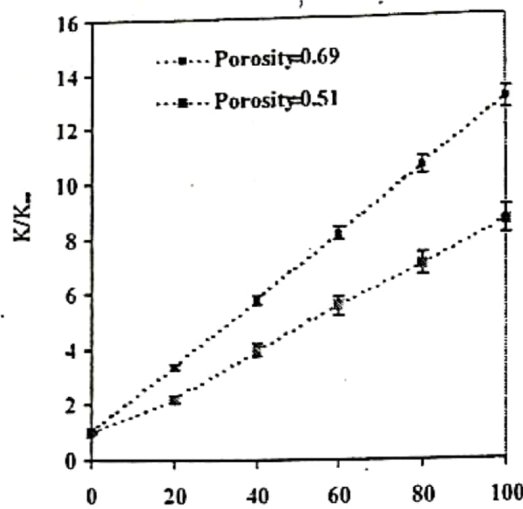


Figure 5. Ratio of permeability of a point with maximum velocity to the bulk permeability versus the nondimensional gap width.

Table 2  
Parameter values of the permeability exponential model

Case	Porosity %	$\alpha \sqrt{K_{\infty}}/b$	$\frac{b\beta\sqrt{K_{\infty}}}{H} \times 10^2$	$\frac{b\beta\sqrt{K_{\infty}}}{H(1-\epsilon_{\infty})} \times 10^2$
E-glass uni I	69	0.171 ± 0.9	0.301 ± 0.05	0.965
E-glass uni II	51	0.169 ± 0.05	0.472 ± 0.04	0.965
average	-	0.17	-	0.965

model, the value of  $K_g/K_{\infty}$  versus  $b/\sqrt{K_{\infty}}$  was plotted. As the air gap width becomes small,  $K_g$  will approach  $K_{\infty}$ . Therefore,  $K_g/K_{\infty}$  was assigned a value of 1.0 for a non-dimensional gap width of zero in each group of data points. Also, the ratio of  $K_g/K_{\infty}$  related to a higher volume fraction is bigger than this ratio for a smaller volume fraction for the same air gap width. The model was solved for different parameter values around the predicted parameters, and then, by comparing the numerical and experimental results, suitable coefficients values were chosen.

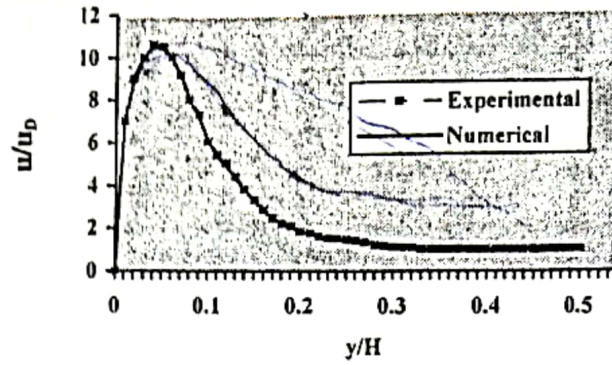
Figure 6 shows the comparison between the experimental and numerical results for the effect of Reynolds number on the velocity profile. The results are presented for Reynolds numbers 0.03, 0.1, and 0.2. As can be seen, the decrease in maximum values of  $u/u_D$  are due to the increase in Reynolds numbers.

Parameters of the predictive exponential model for permeability have been evaluated from the experimental results. These values for two types of fibers are presented in Table 2.

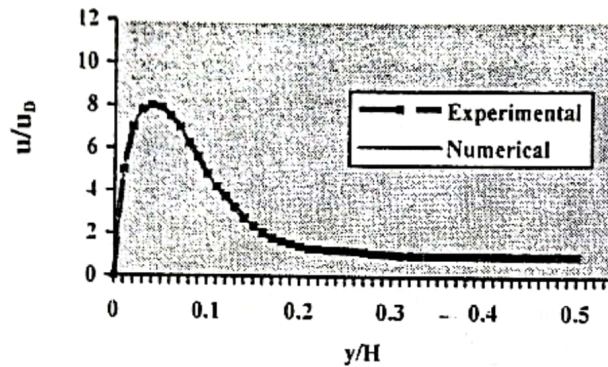
As a result, the final form of the variable permeability function is presented as follows:

$$K = K_{\infty} \left( 1 + \frac{0.17b}{\sqrt{K_{\infty}}} \exp \left( -\frac{0.00965(1-\epsilon_{\infty})y}{(b/H)\sqrt{K_{\infty}}} \right) \right)$$

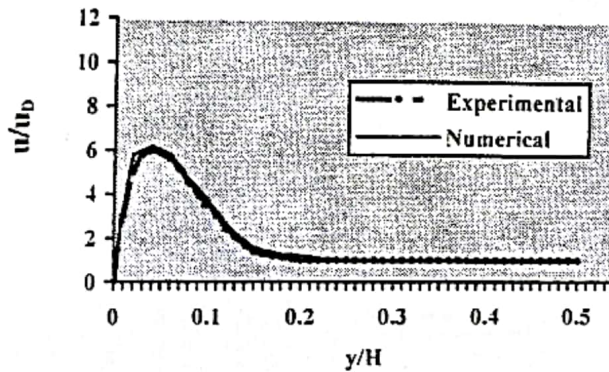
Figure 7a shows the effect of the bulk variable porosity, with constant air gap and constant Reynolds number, on the velocity profile obtained from the experimental result. Figure 7b shows the same effect relating to the numerical results. Also, based on the assumed model, the effect of the air gap width on the velocity profile was investigated



(a)



(b)

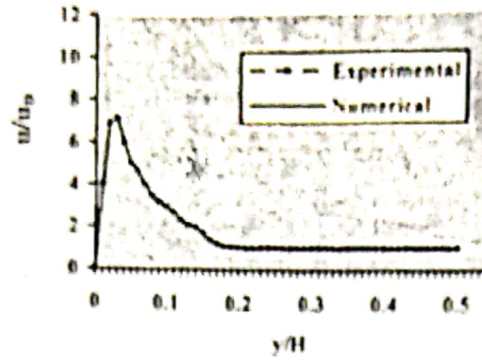


(c)

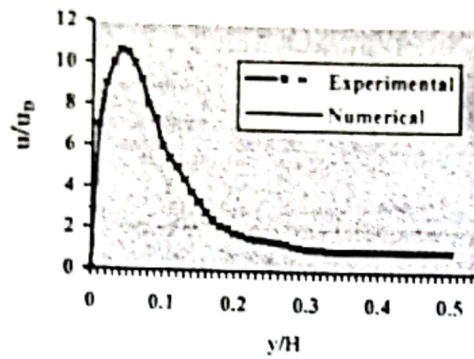
Figure 6. Effect of Reynolds number variation on the velocity fluid flow: a)  $Re = 0.03$ , b)  $Re = 0.1$ , and c)  $Re = 0.2$

using numerical results, which are shown in Fig. 8. As seen from the above-mentioned figures, the variation in free-stream porosity has a significant effect on the flow field. Also, different values of the air gap length generate different permeability from the walls. The air can also cause a

higher porosity at the boundary regions. The larger air gap width causes an increase in the maximum value of the velocity ratio ( $u/u_D$ ); also, the increase in the bandwidth of the nonuniformity of flow.



(a)



(b)

Figure 7. Effect of bulk porosity on the velocity profile: a) porosity = 0.69 and b) porosity = 0.51.

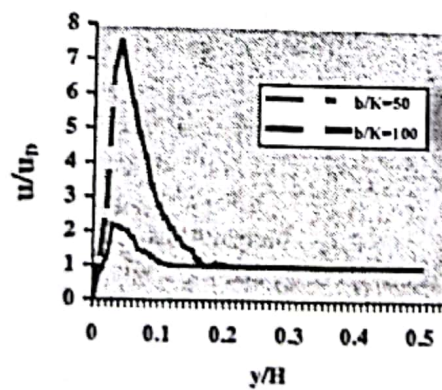


Figure 8. Effect of air gap width on the velocity profile.



## 6. CONCLUSION

The purpose of the present study is to show the nature and importance of the channeling effect and its influence on flow through a medium with variable porosity, with the aid of experimental investigation.

An exponential model to consider the channeling effect was assumed in order to enable the prediction of free surface enhancement in fluid flow through porous media. The model parameters were evaluated by experimental tests for two types of preformed fibers and different pressure gradients and air gaps between the mold walls and fiber edges.

It was found that the results had good convergence. Also, based on this model, the numerical solution of the governing equations produced suitable results to describe the effect of the Reynolds number and the gap width on the velocity profile.

The study was completed by comparing the numerical results of the Reynolds number effect and the air gap width on the velocity profile, with that of the experimental results for the same effects.

Finally, results were verified by the exponential model for permeability prediction in a nonhomogeneous media.

## REFERENCES

Benenati, R. F., and Brosilow, C. B., Void fraction distribution in beds of spheres, *AIChE J.*, vol. 4, pp. 450-464, 1962.

Bickerton, S., and Advani, S. G., Characterization of corner and edge permeability during mold filling in resin transfer molding, *1995 Recent Advances Composite Materials*, ASME, New York, vol. 56, pp. 143-150, 1995.

Chen, S. C., and Vafai, K., Analysis of free surface momentum and energy transport in porous media, *Numer. Heat Transfer*, vol. 29, pp. 231-296, 1996.

Roblee, L. H. S., Baird, R. M., and Tierreg, J. W., Radial porosity variation in packed beds, *AIChE J.*, vol. 8(3), pp. 359-361, 1958.

Schertz, W. M., and Bischoff, K. B., Thermal and material transport in non-isothermal packed bed, *AIChE J.*, vol. 15, pp. 597-604, 1969.

Schwartz, C. E., and Smith, J. M., Flow distribution in packed beds, *Ind. Eng. Chem.* vol. 45, pp. 1209-1218, 1953.

Shahnazari, M. R., and Abbassi, A., Analysis of free surface enhancement in a media with variable porosity, *J. Porous Media*, vol. 7, pp. 1-7, 2004.

Srinivasan, V., and Vafai, K., Analysis of linear enhancement in two-immiscible fluid system in porous medium, *ASME J. Fluids Eng.*, vol. 116, pp. 135-139, 1994.

Vafai, K., Analysis of channeling in variable porosity media, *ASME J. Energy Resources Technol.*, vol. 108, pp. 131-139, 1986.

Yoon, M. K., Barooah, A. P., Berker, B., and Sun, Q., Permeability and porosity estimation in resin transfer molding process, *J. Mater. Process. Manuf. Sci.*, vol. 7, pp. 173-184, 1998.

## APPENDIX: PERMEABILITY ESTIMATION METHOD

The governing equations for Newtonian, incompressible, laminar, inertia-free, and free-of-entrance effects are as follows:

$$\frac{\partial u}{\partial x} = 0 \quad u = \frac{-K}{\mu} \frac{\partial p}{\partial x} \quad u = \varepsilon \frac{dx}{dt} \quad Q = \varepsilon \frac{dx}{dt} A \quad \varepsilon \frac{dx}{dt} = \frac{\bar{K}}{\mu} \frac{\Delta P}{x}$$

where  $u$  is the Darcy velocity,  $x$  is the local coordinate,  $K$  is the preformed fibers' permeability,  $\mu$  is fluid viscosity,  $p$  is the pressure,  $dx/dt$  is the flow front velocity,  $\varepsilon$  is the porosity,  $Q$  is the flow rate, and  $A$  is the cross-sectional area.

### Direct Method

Equations in the previous section are discretized with a first-order finite difference approximation

$$x_k - x_{k-1} = \frac{\Delta t_k}{\varepsilon_k A} Q \quad x_k - x_{k-1} = \frac{\bar{K}_k \Delta t_k \Delta P_k}{\varepsilon_k \mu}$$

### Adaptive Method

By re-arranging the above-mentioned equations, it follows that

$$Q_k = \varepsilon_k (x_k - x_{k-1}) A / \Delta t_k \quad x_k = \bar{K}_k (\Delta P)_k A / (\mu Q_k)$$

and a pre-defined output signal vector  $C_k$ , a parameter vector  $B_k$ , and an input matrix  $A_k$  can results as

$$C_k = \{Q_k, x_k, \mu (x_k - x_{k-1}) Q_k Q_{k-1}\}$$

$$B_k = [\varepsilon_k, \bar{K}_k, K_k]$$

$$A_k = \begin{bmatrix} (x_k - x_{k-1}) A / \Delta t_k & 0 & 0 \\ 0 & \Delta P_k A / (\mu Q_k) & 0 \\ 0 & 0 & A [Q_{k1} \Delta P_k - Q_k \Delta P_{k-1}] \end{bmatrix}$$

$$C_k = A_k B_k$$